Simultaneous nitrogen and dissolved methane removal from an upflow anaerobic sludge blanket reactor effluent using an integrated fixed-film activated sludge system

T. Allegue, M.N. Carballo-Costa, N. Fernandez-Gonzalez, J.M. Garrido

Accepted Manuscript

How to cite:
Journal of Environmental Management, 263 (2020), 110395.
doi: 10.1016/j.jenvman.2020.110395

Simultaneous nitrogen and dissolved methane removal from a upflow anaerobic sludge blanket reactor effluent using an integrated fixed film activated sludge system

T. Allegue*, M.N. Carballo-Costa, N. Fernandez-Gonzalez and J.M. Garrido.

Department of Chemical Engineering, School of Engineering, University of Santiago de Compostela, Campus Vida, E-15782, Santiago de Compostela, Spain (tomas.allegue@usc.es, nievescarballoc@gmail.com, nuria.fernandez.gonzalez@uva.es, juanmanuel.garrido@usc.es).

*Corresponding author. Tel.: +34881816741.

Authors' affiliations and contact details:

Tomás Allegue, María Nieves Carballo-Costa, Nuria Fernandez-Gonzalez and Juan M. Garrido

Affiliation: University of Santiago de Compostela, Department of Chemical Engineering, School of Engineering, E-15782, Santiago de Compostela, Spain

E-mail: tomas.allegue@usc.es; nievescarballoc@gmail.com; nuria.fernandez.gonzalez@uva.es; juanm.garrido@usc.es

Tel: +34 881 816 741

Highlights

- Up to 32.5 mg TN L^{-1} and 93% of the dissolved CH_4 were removed in the IFAS system.
- Suspended biomass was completely washed-out from the IFAS system.
- Biofilm carriers played a key role in nitrogen and CH_4 removals.
- Almost half of the CH_4 and nitrogen removals were observed in the aerobic stage.
- Aerobic methanotrophs and anammox were detected in the anoxic and aerobic compartments.

Keywords

Upflow anaerobic sludge blanket; Methane oxidation; Denitrification; Integrated fixed-film activated sludge; Biofilm carriers; Greenhouse gas.

Abbreviations

AMO-D: aerobic methane oxidation coupled to denitrification

Anammox: anaerobic ammonium oxidation

$COD_{S:}$ soluble chemical oxygen demand

COD_T: total chemical oxygen demand

DO: dissolved oxygen

FA: Free ammonia

GHG: greenhouse gas

HYME-D: hypoxic methane oxidation coupled to denitrification

IFAS: Integrated fixed-film activated sludge

MBR: membrane bioreactor

MLTSS: mixed liquor total suspended solids

MLVSS: mixed liquor volatile suspended solids concentration

MRR: methane removal rate

N-damo archaea: nitrate-dependent anaerobic methane oxidation archaea

N-damo bacteria: nitrite-dependent anaerobic methane oxidation bacteria

NOB: nitrite-oxidizing bacteria

NRR: nitrogen removal rate

OLR: organic loading rate

R: recycling ratio

TN: total nitrogen

UASB: upflow anaerobic sludge blanket

1. Introduction

Anaerobic wastewater treatment technologies are widely used in warm climate countries for treating low-strength streams at room temperature. Indeed, there are hundreds of upflow anaerobic sludge blanket (UASB) reactors operating in different parts of (semi)tropical regions due to low or even zero energy demand (Chernicharo et al., 2015). One of the main constraints of the UASB technology is related to its insufficient removal of organic matter and nitrogen. Given the low C/N ratios commonly observed in anaerobic effluents, the addition of expensive external carbon sources (e.g., ethanol and methanol) is frequently necessary to improve nitrogen removal through heterotrophic denitrification processes. In addition, Noyola et al. (2006) estimated that up to 50% of the methane produced in methanogenic reactors that treat domestic sewage at 20 °C could remain dissolved in their effluents. Methane is a strong greenhouse gas

(GHG) with a global warming potential 28 times higher than CO_2 for a hundred year time horizon (Myhre et al., 2013), which contributes to aggravate the climate change problem. However, this dissolved methane present in UASB effluents can be biologically used as an inexpensive electron donor to denitrify to reduce both GHG emissions and nitrogen content of the treated wastewater. So far, different simultaneous nitrogen and methane removal bioprocesses are distinguished. First, in aerobic methane oxidation coupled to denitrification (AMO-D), strict aerobic methanotrophs oxidize methane into methane oxidation products (Modin et al., 2007). Afterward, conventional heterotrophic denitrifiers can use these oxidation products as an electron donor to reduce nitrate and/or nitrite to dinitrogen gas (Equations 1 and 2). Second, in the anaerobic pathway two main microorganisms are involved: nitrate-dependent anaerobic methane oxidizers (n-damo archaea), such as "*Candidatus* Methanoperedens nitroreducens" (Haroon et al., 2013), which are able to reduce nitrate to nitrite using methane as electron donor (Equation 3), and nitrite-dependent anaerobic methane oxidizers (n-damo bacteria), such as "*Candidatus* Methylomirabilis oxyfera" (Ettwig et al., 2010), which are able to reduce nitrite to dinitrogen gas using also methane as electron donor (Equation 4). Third, Cao et al. (2019) also demonstrated an innovative pathway for removing methane and nitrogen in extreme oxygen-limited conditions, which consist of hypoxic methane oxidation coupled to denitrification (HYME-D), where, instead of using oxygen as the final electron acceptor, aerobic methanotrophs directly utilize nitrate as electron acceptor to oxidize methane and produce organic compounds that could be subsequently utilized by conventional heterotrophic denitrifiers to denitrify.

$$5CH_4 + 5O_2 + 4NO_3^- + 4H^+ \rightarrow 2N_2 + 12H_2O + 5CO_2 \quad (1)$$

$$3CH_4 + 3O_2 + 4NO_2^- + 4H^+ \rightarrow 2N_2 + 8H_2O + 3CO_2 \quad (2)$$

$$2CH_4 + 8NO_3^- \rightarrow 2CO_2 + 8NO_2^- + 4H_2O \quad (3)$$

$$3CH_4 + 8NO_2^- + 8H^+ \rightarrow 3CO_2 + 4N_2 + 10H_2O \quad (4)$$

Therefore, to minimize the environmental impact of effluents from UASB reactors that treat low-strength sewage at room temperature, and to comply with the increasingly severe effluent discharge regulations, further low-footprint post-treatment systems are required. On this ground, authors such as Kampman et al. (2012), Cai et al. (2015), Pelaz et al. (2017), and van Kessel et al. (2018) proposed the use of dissolved methane as an inexpensive electron donor to denitrify. In previous studies carried out in our laboratories, a hybrid MBR system was proposed as an alternative post-treatment system to minimize the impact of effluents from UASB reactors that treat domestic sewage at room temperature (Silva-Teira et al., 2017; Alvarino et al., 2019). In the present research, the same idea of using dissolved methane as an electron donor to denitrify is considered. However, the utilization of an integrated fixed-film activated sludge (IFAS) with a secondary settler instead of a membrane bioreactor (MBR) system was evaluated. Unlike the MBR technology, which requires a high energy demand associated with membrane operation, IFAS systems can result in a less-energy consuming alternative, but probably with lower effluent quality. The use of biofilm technologies such as the IFAS system, which combines the use of both attached and suspended biomass, has arisen as an alternative for the treatment of domestic or industrial sewage, leading to more compact systems than the conventional activated sludge ones. The IFAS technology enables to increase the effective biomass concentration, improving biomass diversity without the need to enlarge the size of the different compartments of treatment plants. Furthermore, biofilm carriers enhance the retention of slow-growth microorganisms, such as nitrifiers (Randall and Sen, 1996) or aerobic/anaerobic methane oxidizers, preventing them from being washed out through

the IFAS final effluent. Besides, biofilms are spatially heterogeneous, which makes possible the coexistence of anaerobic, anoxic, and aerobic bioprocesses in them (Leyva-Díaz et al., 2016).

The present study aims to evaluate the feasibility of using an IFAS system as an alternative post-treatment technology to mitigate the environmental impact of two of the main pollutants present in UASB effluents, such as dissolved methane and nitrogen. To this end, a low-footprint bench-scale plant (186 L), made up of a UASB (120 L) followed by an IFAS (66 L) system, was operated. In a previous study, within the same integrated system operation, Arias et al. (2018) analyzed the removal efficiencies achieved for a wide range of organic micropollutants. However, in the present study, special attention was given to the suspended biomass retention capacity and the potential for removal of dissolved methane and nitrogen removal of the IFAS post-treatment system. Furthermore, the role of carriers in the processes of denitrification and nitrification and the microbial communities present in the biofilm were also analyzed. Finally, the results achieved in this research were compared with previous studies, where similar operating conditions were applied (Silva-Teira et al., 2017; Alvarino et al., 2019). Nevertheless, instead of using an IFAS, a hybrid MBR was proposed as a post-treatment alternative to treat effluents from UASB reactors.

2. Materials and methods

2.1 Reactor configuration and operation

A 186 L pilot plant (Figures 1 and S1) was used for 407 days in order to treat domestic sewage at room temperature. The pilot plant was first composed of a 120 L methanogenic reactor, using the UASB configuration with granular sludge. The obtained UASB effluent was subsequently led to a pre-anoxic IFAS system composed

of three different compartments: a first anoxic compartment (36 L) with mechanical mixing, in which simultaneous nitrogen and methane removal bioprocesses were intended, using suspended biomass and also biomass attached to polyurethane sponge biofilm carriers (Levapor); a second aerobic compartment (20 L), where ammonium oxidation processes were carried out, with the presence of suspended biomass and biofilm adhered to rigid polyethylene supports (Biochip). Both biofilm carriers were moved freely in the liquid volume of the anoxic and aerobic compartments, respectively; and finally, a settler (10 L) in which the physical biomass/effluent separation was carried out. Moreover, the system operation was controlled by a PLC Micrologix (Allen-Bradley) connected to a computer.

Three different types of biomass conformation (granular, attached to carriers, and suspended) and three redox conditions (anaerobic, anoxic, and aerobic) were present in the suggested integrated system. The two different biofilm carriers used, Levapor and Biochip (Figure S2), presented an external specific surface of 486 and 2,174 m^2 m^{-3}, and a volume of 2.8×10^{-3} and 4.15×10^{-4} L, respectively. The amount of carrier used for both varied throughout the experimentation period. The initial apparent volume percentage for Levapor was of 20%. However, this value was raised up to 23% on day 250. As a consequence of the higher difficulty in keeping Biochip carriers homogenously mixed, the initial apparent volume percentage was only 7%. Nevertheless, this value was stepwise increased to 12, 16, and 19% on days 135, 247, and 309, respectively. Biochip was utilized in the aerobic compartment, instead of Levapor, due to its 4.47 times higher external specific surface, which favors the nitrifying capacity per unit of carrier volume, where oxygen transfer usually limits biological conversions (Henze et al., 2002). Conversely, Levapor carriers were used in

the anoxic compartment because of their higher void volume, which could favor the development of anaerobic environments.

The UASB was continuously fed with synthetic wastewater, mimicking a typical composition for domestic sewage: skimmed milk (diluted with tap water); $NaHCO_3$ (960 mg L^{-1}); NH_4Cl (18 mg N L^{-1}) and trace elements with the same composition as proposed by Silva-Teira et al. (2017). The UASB-IFAS integrated system was continuously fed with a fixed sewage flow of 140 L d^{-1}, which resulted in hydraulic retention times (HRT) of 21 h and 10 h for the UASB and the IFAS system, respectively. Two different recirculation streams were applied in the post-treatment system: an internal recycling ratio (R) of 1.5 was applied from the aerobic to the anoxic compartment to provide an electron acceptor, and an external recirculation from the settler to the anoxic chamber to return the activated sludge to the post-treatment system (R = 1.5). Therefore, a total recirculation value of 3 was fixed throughout the operation. This crucial parameter also governs the contact time in each post-treatment compartment and the quantity of O_2 that is recycled to the anoxic compartment. The UASB reactor was inoculated with active biomass from the brewery industry, while the post-treatment system was seeded using stored flocculent biomass obtained from the MBR post-treatment system operated by Silva-Teira et al. (2017).

Two main periods were distinguished during this study. In Period I (days 0–167), suspended and attached-to-carriers biomass were observed in the IFAS post-treatment system. Period II (days 168-407) was characterized by the presence of only attached-to-carriers biomass because all the suspended biomass was unintentionally washed out from the IFAS system.

2.2 Batch tests experimental procedure

In order to better understand the processes of denitrification and oxidation of methane in the proposed IFAS system, batch assays were performed in 500 mL flasks on day 407, using only biofilm adhered to Biochip and Levapor biofilm carriers. Thus, biomass conditions were specific to that given period. Processes such as anaerobic ammonium oxidation (anammox; $NH_4^+ + NO_2^-$), conventional heterotrophic denitrification (Acetate + NO_3^-), and anaerobic methane oxidation coupled to denitrification processes, using nitrate and nitrite ($CH_4 + NO_3^-/NO_2^-$) as electron acceptors, were evaluated. Levapor and Biochip biofilm carriers were extracted from the anoxic and aerobic compartments of the IFAS system, respectively. In the Levapor assays, the flasks were filled with 324 mL of a phosphate buffer solution (143 mg KH_2PO_4 L^{-1} and 740 mg K_2HPO_4 L^{-1}) and 27 foam biofilm carriers (76 mL of volume, 19% apparent volume). In the Biochip assays, the bottles were filled with 221 biofilm carriers (92 mL of volume, 23% apparent volume) and 302 mL of the same buffer solution. The exact volume capacity of the flask bottles was 539 mL. The biofilm did not detach from the carriers and was washed three times with the phosphate buffer solution to ensure the absence of organic matter or nitrogen species. After adding the carriers into the flask bottles, they were flushed for 5 min with nitrogen or methane, according to the conditions of the tests, to assure anoxic conditions and provide electron donors, respectively. For the $CH_4 + NO_2^-/NO_3^-$ tests, the headspace of the flasks was saturated in CH_4. Stock solutions with NH_4Cl, $NaNO_2$, and $CH_3COONa \cdot 3H_2O$ were prepared. Then, 1 mL of each stock solution was provided to the corresponding bottle at the beginning of the experiment. Ammonium and nitrite concentrations of 20 and 30 mg N L^{-1}, respectively, and COD_T concentrations of 200 mg L^{-1}, were initially added. The flasks were incubated at 25 ºC and shaken at 150 rpm for 8 h. Gas and liquid samples were collected every 2 h through

188 the bottle's septum. The final sample was taken after 23 h. Once liquid samples were
189 taken using a syringe, they were immediately filtered through a 0.45 μm nitrocellulose
190 membrane filter (HA, Millipore). Gas samples were also taken for analysis in the CH_4 +
191 NO_3^-/NO_2^- tests.

192

193 **2.3 Liquid and gas samples analysis**

194 Nitrogen species (nitrite, nitrate, and ammonium), Total (COD_T) and soluble chemical
195 oxygen demand (COD_S), mixed-liquor total and volatile suspended solids (MLTSS and
196 MLVSS), pH, temperature, and oxidation-reduction potential (ORP) were measured
197 according to Standard Methods (Rice et al., 2012). The dissolved oxygen (DO)
198 concentration in both compartments was also periodically measured by a multi-
199 parameter meter (Hach HQ40d), with a luminescent optical probe (IntelliCAL
200 LDO101). Oxygen concentration in the aerobic chamber was not controlled throughout
201 the operation. The dissolved methane concentration in the liquid phase of the anoxic and
202 the aerobic compartments was measured according to the procedure described by
203 Sánchez et al. (2016). A MilliGascounter type MGC-10 (Ritter) was used to measure
204 the biogas production, while the biogas composition, including CO_2, N_2, and CH_4, was
205 analyzed using a gas chromatograph 5890 series II (Hewlett-Packard) with a thermal
206 conductivity detector and a column of Porapack Q 80/100 2 m x 1/8" (SUPELCO), with
207 column and detector temperatures of 34 ºC and 110 ºC, respectively, and helium as
208 carrier gas. All the aforementioned parameters were measured at least twice a week.

209

210 **2.4 DNA extraction and 16S rRNA gene amplicon sequencing**

211 Biomass samples were taken from Levapor packing materials on days 175, 265, and
212 368. Furthermore, the attached biomass composition was also analyzed in Biochip
213 carriers, on day 368. Unfortunately, suspended biomass communities were not
214 evaluated due to complete washing of biomass detected from day 167 onwards.
215 Microbial communities of the two carriers were monitored by sequencing the V3V4 and
216 V2V3 regions of the 16S rRNA gene for bacteria and archaea, respectively. Amplicon
217 libraries, sequencing, and data analysis were performed as described in the
218 Supplementary Material.

219

220 **3 Results and discussion**

221 **3.1 General results**

222 The pilot plant was continuously operated over a period of 407 days, with an average
223 temperature value of 21.1 ± 1.4 ºC. A daily feed flow of 138.3 ± 21.9 L d^{-1} was treated,
224 with COD_T and COD_S concentrations of 891 ± 214 and 782 ± 204 mg COD L^{-1}, which
225 resulted in an average organic loading rate (OLR) of around 1 kg COD m^{-3} d^{-1} (referred
226 to the UASB system). Average HRT values of 21.1 ± 3.1 and 9.8 ± 1.5 h were applied
227 for the UASB and IFAS post-treatment systems, respectively. Considering both the
228 external and internal recirculation in the IFAS system, a constant R of 3 ± 0.6 was
229 applied throughout the operation. A pH value of 7.26 ± 0.26 was observed in the UASB
230 throughout the operation, while values of 7.6 ± 0.1 and 7.9 ± 0.2 were determined in the
231 anoxic and aerobic compartments of the IFAS system, respectively. During the entire
232 experimentation period, a high average COD_T removal efficiency of 93 ± 2% was
233 detected in the first methanogenic stage. From the beginning of the operation, high
234 COD removals were observed in the UASB reactor due to the large amount of anaerobic

235 granules used as inoculum. Approximately 75% of the overall COD inlet was
236 methanized in the UASB reactor, producing a biogas flow of 37.3 ± 8.5 L d^{-1}, with the
237 following composition: 75 ± 2.5% CH_4, 15 ± 2.8% CO_2, and 9 ± 3% N_2. Nevertheless,
238 not all methane produced was present in the gas phase, but 17.6 ± 2.9 mg CH_4 L^{-1}
239 dissolved in the anaerobic effluent were detected, representing the 14 ± 6% of the total
240 methane produced. Low COD_T and COD_S concentrations were detected in the anaerobic
241 effluent, with values of only 57 ± 15 and 43 ± 12 mg COD L^{-1}, respectively, excluding
242 in both measurements the portion related to the dissolved methane COD. This organic
243 matter could be used as an electron donor in the pre-anoxic compartment of the IFAS
244 system, promoting heterotrophic denitrification processes. Nevertheless, COD_T was also
245 detected in the final effluent of the system, at values of 77 ± 21.4 and 53.8 ± 12 mg
246 COD L^{-1}, during Periods I and II, respectively. During Period I, due to the continuous
247 VSS washout in the IFAS system, COD concentrations in the final effluent were even
248 higher than those detected in the UASB effluent. Regarding Period II, COD
249 concentrations in the UASB outlet and in the final effluent were similar. This fact
250 indicates that the biodegradable COD fraction of the UASB effluent is very low.
251 Therefore, conventional heterotrophic denitrifiers, using the remaining COD of the
252 UASB effluent (excluding methane), should have played a minor role in the nitrogen
253 removal processes detected in the IFAS post-treatment system.

254

255 **3.2 Impact of biofilm carriers' addition on the nitrification potential**

256 Most of the total nitrogen (TN) of the UASB effluent was present in the form of
257 ammonium, with an average concentration value of 54 ± 8 mg NH_4^+-N L^{-1} (Figure S3).
258 Oxygen was continuously provided in the aerobic compartment to allow nitrification

processes, and average DO concentration values of 3.2 ± 0.7 and 4.4 ± 0.6 mg O_2 L^{-1} were measured during Periods I and II, respectively.

Whenever the Biochips' apparent volume was higher, the ammonium oxidizing rates, referred to the aerobic compartment, accordingly increased. Average values of 157.1 ± 61.5, 165.4 ± 34.7, 191.5 ± 47.9, and 240.6 ± 55.5 mg NH_4^+-N L^{-1} d^{-1} were attained for the aforementioned periods, respectively (Figure S4). Nevertheless, despite the supports addition, full ammonium oxidation was not accomplished during the study and concentrations of 25.3 ± 12.3, 23.2 ± 5.2, 23.2 ± 6.7, and 19.3 ± 6.5 mg NH_4^+-N L^{-1} were measured (Figure S5). During Period II, the ammonia consumption rate referred per unit of suspended carrier surface was of 0.59 ± 0.15 g NH_4^+-N m^{-2} d^{-1}.

Although the suspended biomass was totally washed-out from the IFAS system on day 167, significant ammonium oxidation rates were achieved during Period II (without the presence of suspended biomass in the IFAS system), indicating that biofilms were responsible for the removal of ammonium observed. This highlights the essential role of biofilm carriers in nitrification processes. In order to accomplish better nitrification rates, a higher surface area of biofilm carriers is required by increasing either the aerobic compartment volume or the carrier added volume. A second strategy is to generate higher DO concentrations in the aerobic compartment, which is usually the limiting substrate in biofilm processes.

Partial nitritation processes were observed in the aerobic compartment during most of Period I. In fact, throughout the first 119 days of operation, nitrite was the main available electron acceptor, with an average concentration of 3.5 ± 1.5 mg NO_2^--N L^{-1} (Figure S5).

From that day onwards, the nitrite concentration considerably declined due to the nitrite-oxidizing bacteria (NOB) activation. As a result, nitrate became the most

abundant oxidized nitrogen species in the aerobic stage. During most of Period I, the estimated average free ammonia (FA) concentration of 0.81 mg NH_3-N L^{-1} may have partially inhibited the NOB activity. It has been reported in the literature that FA values between 0.1 and 1.0 mg NH_3-N L^{-1} I initiated the inhibition of NOB activity (Anthonisen et al., 1976). Nevertheless, over time, the biomass colonization of the packing media could have provided a more suitable environment for NOB activity to tolerate the inhibitory effect of FA (Villaverde et al., 2000). During Period II, a nitrite concentration of only 0.25 ± 0.17 mg NO_2^--N L^{-1} was detected.

3.3 Suspended biomass washout in the IFAS system

One of the main concerns of the present study was related to the suspended biomass retention capacity of the IFAS system when treating low-C/N ratio UASB effluents, mainly due to the reports regarding the poor settling properties of suspended biomass when treating effluents with these characteristics (Metcalf & Eddy et al., 2013). At the beginning of the operation, the MLTSS and MLVSS concentrations measured in the pre-anoxic compartment were of 3.5 and 3.1 g L^{-1} (Figure 2), respectively.

Nevertheless, from day 47 to 89, as a consequence of the low mixing in the anoxic compartment, large amounts of biomass gradually accumulated in the bottom part, resulting in a dramatic drop in the suspended solids concentration. Once the mechanical mixing was increased on day 83, the mixed liquor was immediately resuspended, obtaining a homogeneous mixture, which increased the MLVSS concentration. Between days 109 and 167, the MLVSS concentration declined in the IFAs system from 2.62 to only 0.05 g L^{-1}. During that period, sludge washout was observed in the effluent of the IFAS system, with MLTSS and MLVSS concentrations of approximately 61 ± 11 and 45 ± 12 mg L^{-1}, respectively. The average liquid up-flow velocity in the settler

compartment was 0.31 m^3 m^{-2} h^{-1} throughout the entire operation. Curiously, the biomass washout was concomitant with the period in which nitrite began to oxidize in the aerobic compartment, making nitrate the main electron acceptor. From day 167 onwards, the MLTSS and MLVSS observed in the final effluent were around 39.9 ± 11.4 and 33.7 ± 9 mg L^{-1}, respectively. Once all suspended biomass was totally removed from the IFAS post-treatment system (Period II), the role of biofilm carriers in nitrogen and methane removal-processes was thoroughly studied.

The low average OLR applied to the IFAS system throughout the entire operation, 0.14 kg COD m^{-3} d^{-1}, and the poor organic removal rate observed in the IFAS system due to the low biodegradable COD content of the UASB effluent could be the main causes responsible for the biomass washout. Consequently, the only way of treating these kinds of anaerobic effluents with low C/N ratios is by promoting biofilm growth adhered to supports. Therefore, if the complete retention of suspended biomass is intended, a pre-anoxic MBR system, such as that done by Alvarino et al. (2019), must be used.

3.4 Methane removal in the IFAS post-treatment system

Methane removals in the anoxic compartment of the IFAS system were calculated using mass balances (Supplementary Material). During Period I, an upward trend in methane removal was clearly observed, attaining a maximum volumetric methane removal rate (MRR) and methane removal efficiency of 52.5 mg CH_4 L^{-1} d^{-1} and 72.7% on day 126, respectively (Figure 3), both values referred only to the anoxic compartment. Nevertheless, once the suspended biomass from the IFAS system was lost, and nitrate became the main electron acceptor detected, methane removals significantly dropped into the anoxic compartment. During Period II, values of 23.9 ± 10.4 mg CH4 L^{-1} d^{-1} and 36.6 ± 10.5% were attained, respectively. Thereby, the complete loss of suspended

biomass in the IFAS system led to a reduction of around 50% in both parameters. In spite of the negative effect of the suspended biomass washout, the methane removals detected during Period II, highlight the important role of the adhered biomass in the methane oxidation bioprocesses.

The recirculations applied in the post-treatment system will determine the amount of DO provided to the anoxic compartment, which could cause the proliferation of aerobic methanotrophs. If it is assumed that all oxygen reduced in the anoxic stage during Period I and II, 32.5 ± 9.3 and 41.8 ± 5.9 mg O_2 L^{-1} d^{-1}, respectively, was consumed through aerobic methanotrophs, and considering its stoichiometry (2 g O_2 g^{-1} CH_4; Equations 1 and 2), these microorganisms could explain up to 48% and 87% of the average MRRs observed in the anoxic compartment during Period I and II, respectively. Besides aerobic methane oxidation processes, some other metabolic pathways could be involved, especially during Period I, such as anaerobic methane oxidation and even the possibility of other lesser-studied metabolic pathways, such as the HYME-D suggested by Cao et al. (2019).

In previous studies, Silva-Teira et al. (2017) treating the same type of domestic sewage, under similar operating conditions, but using an MBR instead of an IFAS system, achieved a maximum MRR of 195 ± 17 mg CH_4 L^{-1} d^{-1} in the anoxic compartment. This value is almost four times higher than the maximum attained in the current research (52.5 mg CH_4 L^{-1} d^{-1}). This fact could be attributed to the presence of an ultrafiltration membrane, which ensured the complete retention of suspended biomass in the MBR. Furthermore, they observed that MRRs depended on the applied feed flow, which was approximately three times higher in the previous study (355 L_{feed} d^{-1}) than in the current one (138 L_{feed} d^{-1}). However, the highest methane removal efficiencies observed in the anoxic compartment during this research, with the presence of nitrite and suspended

biomass (78%), were similar to the maximum attained by Silva-Teira et al. (2017). This suggested that the MRR observed during Period I, with the presence of microorganisms growing in biofilms and in suspension, was limited by the hydraulic load applied to the system. During Period II, in which only biofilms were responsible for the methane oxidation, MRRs could be limited by the transfer of either methane or oxygen to the biofilms.

The dissolved methane that was not oxidized in the first anoxic compartment was led to the aerobic one. This methane could be biologically oxidized or stripped-off into the atmosphere. Throughout the entire operation, dissolved methane was detected in the aerobic compartment, with values ranging from 2.10 to 0.01 mg CH_4 L^{-1}. Average concentrations of 0.25 ± 0.2 and 0.32 ± 0.4 mg CH_4 L^{-1} were measured during Periods I and II, respectively. The continuous detection of methane allowed to estimate the amount of this compound that was either desorbed or biologically oxidized in the aerobic compartment (Supplementary Material).

Average MRRs of 53.1 ± 33.4 and 43.5 ± 20.3 mg CH_4 L^{-1} d^{-1} were estimated in the aerobic compartment during Period I and II, respectively. This indicates the crucial role of the aerobic compartment to minimize GHGs emissions from the process. In fact, the average MRRs observed in the aerobic compartment for Period I are similar to the maximum achieved in the anoxic compartment, and almost double the average values achieved during Period II. Considering the methane removals observed in the anoxic compartment and those estimated in the aerobic compartment, high overall removal efficiencies of 89.1 ± 10% and 77 ± 12% were achieved in the whole IFAS post-treatment system during Periods I and II, respectively. The remaining fraction of methane that was not biologically oxidized was considered to be stripped off into the atmosphere. Due to the high oxygen concentration measured in the aerobic

compartment, a high fraction of the methane was surely completely oxidized to carbon dioxide. However, the development of AMO-D processes should not be discarded due to the presence of anoxic environments inside the Biochip.

3.5 Nitrogen removal performance in the IFAs post-treatment system

Similarly, methane mass balances in the anoxic and aerobic compartments, and in the whole IFAS post-treatment system were carried out. An average value of 54 ± 8 mg NH_4^+-N L_{feed}^{-1} was observed in the UASB throughout the research. In order to promote denitrification processes in the anoxic compartment, previous ammonium oxidation into oxidized nitrogen compounds (NO_2^- and NO_3^-) is required. Due to the low organic matter content observed in anaerobic effluents, the use of a coexisting alternative electron donor to denitrify, such as ammonium or dissolved methane, is required to accomplish the denitrification processes. From the beginning of the study, the overall TN removal progressively increased throughout the whole IFAS system, reaching a maximum removal of 32.5 mg TN L_{feed}^{-1} on day 109 (Figure 4). Nevertheless, nitrogen removals dropped between days 126 and 167. This decrease was concomitant to the suspended biomass loss and also with the lower presence of nitrite in the aerobic compartment. However, although only attached biomass was available throughout Period II, an important average nitrogen removal of 18 ± 3.9 mg TN L_{feed}^{-1} was attained. Regarding the nitrogen removal rate (NRR), a maximum value of 119.6 mg TN L^{-1} d^{-1} and an average value of 29.9 ± 17.1 mg TN L^{-1} d^{-1} for Periods and II, respectively, were observed in the first anoxic compartment of the IFAS system. Curiously, denitrification processes were not only restricted to this anoxic compartment but were also continuously detected in the aerobic compartment from the beginning of the study. This fact could be demonstrated because the average TN concentration in the final effluent

409 was 2.9 ± 1.7 mg N L_{feed}^{-1} lower than the measured in the anoxic compartment.
410 Differences in the TN concentrations between these two streams were permanently
411 detected throughout the study (Figure S3). Using mass balances, it was calculated that
412 45.5 ± 24.4 and 54.9 ± 24.2% of the TN removal achieved was surprisingly carried out
413 in the aerobic compartment in the IFAS system during Period I and II, respectively. The
414 existence of different DO concentration gradients, which is characteristic of biofilm
415 systems, may promote anoxic environments in the inner layers of the Biochip carriers,
416 explaining the observed nitrogen removals in the aerobic compartment. This evidences
417 that simultaneous nitrification-denitrification processes were conducted in the Biochip
418 carriers.
419 The COD concentration observed in the final effluent of the post-treatment system was
420 higher or similar than in the UASB effluent. This could indicate a minor role of
421 conventional heterotrophic denitrifiers in the nitrogen removal achieved in the IFAS
422 system. Therefore, other compounds have been alternatively used as an electron donor
423 to denitrify. Part of the nitrogen removal could be explained by means of conventional
424 heterotrophic denitrifiers, using the methane oxidation products produced by aerobic
425 methanotrophs (AMO-D) in the anoxic and aerobic compartments, or by other methane
426 oxidation pathways coupled to denitrification processes, such as anaerobic methane
427 oxidation, or HYME-D. Furthermore, the coexistence of nitrite and ammonium under
428 anoxic conditions could induce the development of anammox microorganisms in the
429 anoxic and aerobic compartments, contributing to improving the nitrogen removals.
430 The maximum nitrogen removals observed in this research (32.5 mg TN L_{feed}^{-1}) were
431 similar to the maximum achieved using a hybrid MBR system (35.1 mg TN L_{feed}^{-1};
432 Alvarino et al., 2019). In both cases, nitrite was present and enhanced nitrogen
433 removals. Furthermore, even without suspended biomass in the IFAs post-treatment

system, high average TN removals were attained (18 ± 3.9 mg TN L_{feed}^{-1})., similar values to those achieved by Silva-Teira et al. (2017; 15 mg TN L_{feed}^{-1}) using the MBR system. In both cases, the nitrite concentration was negligible, with nitrate being the main electron acceptor. Therefore, the current outcomes emphasize the key role performed by the aerobic compartment, with the presence of biofilm carriers, in nitrogen removal processes. It should be emphasized that the use of an IFAS system, with lower MRR, but similar dissolved methane and total nitrogen removal than the MBR system, could be simpler and cheaper, to improve those sewage treatment plants that treat municipal wastewater with UASB systems, as occurs in some warm and temperate countries of the world.

3.6 Microbial community analysis

During Period II, the microbial community was monitored in the two types of free-moving biofilm carriers presented in the reactor (Levapor and Biochip), by means of partial amplicon sequencing of the 16S rRNA gene. Three samples of the attached biomass in Levapor (operating days 175, 265, and 368) and a sample of the Biochip (day 368) biomass were analyzed. Due to the observed biomass washout, suspended biomass could not be studied. On days 175, 265, and 368, several aerobic methanotrophs (*Methylomonas*, *Methylocaldum*, *Crenotrix*, *Methylosiuns*, and a putative methanotroph from the *Methylococcales* order) were detected in Levapor carriers with total relative abundances of 3.20, 3.48, and 2.90%, respectively (Figure 5a). On day 368, its total relative abundance in Biochip carriers was even higher (7.40%), which could explain the high methane removals observed in the aerobic compartment of the IFAS system.

458 In contrast, n-damo bacteria (*Ca*. Methylomirabilis) were only detected in Levapor
459 carriers (anoxic compartment) in the last days of operation (day 368), with a relative
460 abundance of 0.02%, while n-damo archaea were not detected. Biochips carriers were
461 quite enriched in nitrifying organisms during the last days of operation when more than
462 10% of the bacteria belonged to *Nitrospira* genus (Figure 5b). Furthermore, ammonium-
463 oxidizing bacteria of the *Nitrosomonadaceae* family were detected in Biochip carriers
464 with a relative abundance of 3%. As ammonia and low concentrations of nitrite were
465 available, conditions for the growth of anammox bacteria were present in the system.
466 Indeed, *Ca*. Brocadia was present with a relative abundance of 0.03%, 1.20%, and
467 3.18% in Levapor carriers on days 175, 265, and 368, respectively, and with a relative
468 abundance of 6.5% in Biochip carriers on day 368. During Period II, the rest of the
469 community was composed mostly of bacterial families of heterotrophs considered
470 saprophytic microorganisms, such as *Saprospiraceae* or *Moraxellaceae* (Martins and
471 Carreira, 2014). There also species able to carry out nitrate reduction, such as the
472 *Comamonadaceae* family, although their relative abundance decreased through the
473 operation of the IFAS system (Figure 6a). Most Archaea present in both, Levapor and
474 Biochip, were well known methanogenic genera, such as *Methanosaeta*, *Candidatus*
475 Methanoregula, *Methanobacterium*, and *Methanomethylovorans*, among others (Figure
476 6b).
477 These data indicated that during Period II, methane removal was surely achieved in both
478 compartments of the IFAS system through aerobic methanotrophs. Meanwhile, the
479 nitrogen removals observed in Levapor carriers could have been carried out by
480 anammox bacteria or conventional heterotrophic denitrifiers that use methane oxidation
481 products released by aerobic methanotrophs. Moreover, the consortium of nitrifying and

anammox bacteria probably contributed to the nitrogen removals observed in the adhered-to-Biochip biomass.

3.7 Batch assays

Batch experiments were performed under anaerobic conditions at the end of Period II to determine whether anaerobic ammonium oxidation (anammox), conventional heterotrophic denitrification, and anaerobic methane oxidation along with denitrification processes were feasible in both biofilm media carriers (Levapor and Biochip). The batch experiments containing NO_2^- and NH_4^+ in the liquid, and N_2 in the gas phase, showed high denitrification in both carriers' media. Regarding Levapor, high volumetric NRRs of 80.1 and 52.8 mg N L^{-1} d^{-1} for nitrite and ammonium were observed, respectively (Figure 7a). The resulting NO_2^--N/NH_4^+-N ratio (1.5) is similar to that required for the anammox process (1.32). The nitrite and ammonium removal rates per unit of Levapor surface were 0.87 and 0.58 g N m^{-2} d^{-1}, respectively (Table 1).

Table 1. Nitrogen removal rates per unit of Levapor and Biochip surface for the different batch tests.

Batch test (type)	Nitrogen removal rate (g N m^{-2} d^{-1})	
	Levapor	**Biochip**
NO_2^- + NH_4^+	NO_2^--N: 0.87 NH_4^+-N: 0.58	NO_2^--N: 0.49 NH_4^+-N: 0.29
Acetate + NO_3^-	0.83	0.27
CH_4 + NO_3^-	0.17	-
CH_4 + NO_2^-	0.29	-

In the Biochip carriers, higher volumetric NRRs were observed. In fact, nitrite was totally consumed in less than 4 h. Given the lack of nitrite as electron acceptor between 4 and 23 h, the ammonium concentrations remained constant with values of around 10.5 mg N L^{-1} (Figure 7b). The maximum volumetric removal rates of nitrite and ammonium achieved were 246.2 and 142.4 mg N L^{-1} d^{-1}, respectively. The nitrite and ammonium surface removal rates for Biochip carriers were 0.49 and 0.29 g N m^{-2} d^{-1}, respectively. Therefore, the presence of anammox processes in both biofilm carriers' media was clearly confirmed and even with remarkable activities.

With respect to the conventional heterotrophic denitrification tests using acetate as electron donor, nitrate removal rates of 75.9 and 137.5 mg NO_3^--N L^{-1} d^{-1} were achieved for Levapor and Biochip, respectively (Figures 7c and 7d). The nitrate removal rates per unit of support surface were 0.83 and 0.27 g NO_3^--N m^{-2} d^{-1}, respectively. These results pointed out the presence of conventional heterotrophic denitrification processes in both biofilm carriers. However, the low concentration of organic matter provided to the IFAs post-treatment system possibly limited the denitrification rates achieved during the continuous operation.

In the anaerobic methane oxidation tests performed only with Levapor carriers and using nitrate as an electron acceptor, a low NRR of 15.7 mg NO_3^--N L^{-1} d^{-1} was observed (Figure 7e), which corresponds to a removal rate per unit of Levapor surface of 0.17 g NO_3^--N m^{-2} d^{-1}. At the same time, using nitrite as an electron acceptor instead of nitrate, removal rate values of 22.6 mg NO_2^--N L^{-1} d^{-1} and 0.29 g NO_2^--N m^{-2} d^{-1} were attained (Figure 7f). Therefore, the NRRs achieved using nitrite as an electron acceptor were 1.44 times higher than for nitrate. For the nitrate test, if the total CH_4 and NO_3^--N consumed are considered, a ratio of 0.61 mol CH_4 mol^{-1} NO_3^--N was attained. Regarding the nitrite tests, the same ratio was achieved (0.61 mol CH_4 mol^{-1} NO_2^--N).

These ratios are similar to those of anaerobic methane oxidation or HYME-D processes (Cao et al., 2019).

4. Conclusions

The feasibility of using an IFAS system as a post-treatment alternative to mitigate the environmental impact of UASB treating sewage, in terms of greenhouse gas emissions and nutrients, was evaluated. High overall COD removal efficiencies were achieved during the whole experimentation period, with COD_T concentrations in the final effluent that never exceeded 77 mg L^{-1}. Regarding ammonium removal, an average 57 ± 15.7% was achieved. The accomplished ammonium oxidation rates were improved by the gradual addition of Biochip carriers in the aerobic compartment. Therefore, a larger volume of the aerobic compartment, a higher biofilm carrier surface, or higher DO concentrations would have been required in order to achieve complete nitrification.

The maximum nitrogen removal and methane removal efficiencies achieved throughout the IFAS system, 32.5 mg TN L_{feed}^{-1} and around 93%, respectively, were detected during the period in which suspended biomass and nitrite were present. Once the suspended biomass was completely washed out, and nitrate became the main electron acceptor, this value progressively decreased. However, despite the absence of suspended biomass, average nitrogen removals and methane removal efficiencies of 18 ± 3.9 mg TN L_{feed}^{-1} and 77.2 ± 12.2% were attained, respectively, in the IFAS system. Therefore, the use of an IFAS system could be an alternative to reduce the problems related to high nutrient concentrations and greenhouse emissions of UASB systems used in many warm and temperate countries as a secondary sewage treatment method.

During the study, dissolved methane and nitrogen were not only removed in the anoxic compartment, but also in the aerobic one, and with significant importance. The results

obtained pointed out the importance of both biofilm carriers, Levapor and Biochip, in the methane and nitrogen removals observed in the IFAS system. The significant detection in Biochip carriers of aerobic methane oxidizers and *Ca*. Brocadia confirmed the existence of methane and nitrogen removal processes in the aerobic compartment of the IFAS system. Both groups of microorganisms were also detected in the Levapor carriers present in the anoxic compartment.

Acknowledgments

This research was supported by the Ministry of Economy and Competitiveness of Spain through the COMETT project (CTQ2016-80847-R) and by the Ministry of Education and Science of Spain through the Red Novedar project (CTQ2014-51693-REDC). T. Allegue would also like to express his gratitude to the Ministry of Economy and Competitiveness of Spain for awarding a research scholarship (BES-2014-069114). The authors belong to the Galician Network of Environmental Technologies (ED341D R2016/033) and to the CRETUS Strategic Partnership (AGRUP2015/02), financed by the Galician Government.

5. References

Alvarino, T., Allegue, T., Fernandez-Gonzalez, N., Suárez, S., Lema, J.M., Garrido, J.M., Omil, F., 2019. Minimization of dissolved methane, nitrogen and organic micropollutants emissions of effluents from a methanogenic reactor by using a preanoxic MBR post-treatment system. Sci. Total Environ. 671, 165-174. https://doi.org/10.1016/j.scitotenv.2019.03.169 0048-969.

580 Anthonisen, A.C., Loehr, R.C., Prakasam, T.B., Srinath, E.G., 1976. Inhibition of
581 nitrification by ammonia and nitrous acid. J. Water Pollut. Control Fed. 48, 835–852.
582 https://doi.org/ 10.2307/25038971.
583
584 Arias, A., Alvarino, T., Allegue, T., Suárez, S., Garrido, J.M., Omil, F., 2018. An
585 innovative wastewater treatment technology based on UASB and IFAS for cost-efficient
586 macro and micropollutant removal. J. Hazard. Mater. 359, 113–120.
587 https://doi.org/10.1016/j.jhazmat.2018.07.042.
588
589 Cai, C., Hu, S., Guo, J., Shi, Y., Xie, G.J., Yuan, Z., 2015. Nitrate reduction by
590 denitrifying anaerobic methane oxidizing microorganisms can reach a practically useful
591 rate. Water Res. 87, 211–217, https://doi.org/10.1016/j.watres.2015.09.026.
592
593 Cao, Q., Liu, X., Ran, Y., Li, Z., Li, D., 2019. Methane oxidation coupled to
594 denitrification under microaerobic and hypoxic conditions in leach bed bioreactors. Sci.
595 Total Environ. 649, 1-11. https://doi.org/10.1016/j.scitotenv.2018.08.289.
596
597 Chernicharo, C.A.L., Lier, J.B., Noyola, A., Ribeiro, T.B., 2015. Anaerobic sewage
598 treatment: state of the art, constraints and challenges. Rev. Environ. Sci. Bio Tech. 14,
599 649–679. https://doi.org/10.1007/s11157-015-9377-3.
600
601 Ettwig, K.F., Butler, M.K., Le Paslier, D., Pelletier, E., Mangenot, S., Kuypers,
602 M.M.M., Schreiber, F., Dutilh, B.E., Zedelius, J., de Beer, D., Gloerich, J., Wessels,
603 H.J.C.T., van Alen, T., Luesken, F., Wu, M.L., van de Pas-Schoonen, K.T., Op den
604 Camp, H.J.M., Janssen-Megens, E.M., Francoijs, K.J., Stunnenberg, H., Weissenbach,

605 J. Jetten, M.S.M., Strous, M., 2010. Nitrite-driven anaerobic methane oxidation by
606 oxygenic bacteria. Nature 464, 543–548. https://doi.org/10.1038/nature08883.
607
608 Haroon, M.F., Hu, S., Shi, Y., Imelfort, M., Keller, J., Hugenholtz, P., Yuan, Z., Tyson,
609 G.W., 2013. Anaerobic oxidation of methane coupled to nitrate reduction in a novel
610 archaeal lineage. Nature 500(7464), 567-570. https://doi.org/10.1038/nature12375.
611
612 Henze, M., Harremoës P., Jansen J.L.C., Arvin, E., 2002. Wastewater treatment:
613 biological and chemical processes, 3rd edition. Springer, Berlin, Germany.
614
615 Kampman, C., Hendrickx, T.L.G., Luesken, F.A., van Alen, T.A., Op den Camp,
616 H.J.M., Jetten, M.S.M., Zeeman, G., Buisman, C.J.N., Temmink, H., 2012. Enrichment
617 of denitrifying methanotrophic bacteria for application after direct low-temperature
618 anaerobic sewage treatment. J. Hazard. Mater. 227–228. 164–171.
619 https://doi.org/10.1016/j.jhazmat.2012.05.032.
620
621 Leyva-Díaz, J.C., Muñío, M.M., González-López, J., Poyatos, J.M., 2016.
622 Anaerobic/anoxic/oxic configuration in hybrid moving bed biofilm reactor-membrane
623 bioreactor for nutrient removal from municipal wastewater. Ecol. Eng. 91, 449–458.
624 https://doi.org/10.1016/j.ecoleng.2016.03.006.
625
626 Martins, L. and Carreria, V. L., 2014. The Family *Moraxellaceae*. In: Rosenberg, E.,
627 DeLong, E.F., Lory, S., Stackebrandt, E., Thompson, F. (Eds.), The Prokaryotes –
628 *Gammaproteobacteria*. Springer, Berlin, Germany, pp. 443-476.
629

630 Metcalf & Eddy, Inc., Tchobanoglous, G., Stensel, H.D., Tsuchihashi, R., Burton, F.,
631 2013. Wastewater Engineering: Treatment and Resource Recovery, 5th edition.
632 McGraw-Hill Education, New York, USA.
633
634 Modin, O., Fukushi, K., Yamamoto, K., 2007. Denitrification with methane as external
635 carbon source. Water Res. 41, 2726–2738. https://doi.org/10.1016/j.watres.2007.02.053.
636
637 Myhre, G., Shindell, D., Bréon, F.M., Collins, W., Fuglestvedt, J., Huang, J., Koch, D.,
638 Lamarque, J.F., Lee, D., Mendoza, B., Nakajima, T., Robock, A., Stephens, G.,
639 Takemura, T., Zhang, H., 2013. Anthropogenic and natural radiative forcing. In:
640 Stocker, T.F., Qin, D., Plattner, G.K., Tignor, M., Allen, S.K., Boschung, J., Nauels, A.,
641 Xia, Y., Bex, V., Midgley, P.M. (Eds.), Climate change 2013: The Physical Science
642 Basis. Contribution of Working Group I to the Fifth Assessment Report of the
643 Intergovernmental Panel on Climate Change. Cambridge University Press, Cambridge,
644 United Kingdom and New York, NY, USA, pp. 659-740.
645
646 Noyola, A., Morgan-Sagastume, J.M., López-Hernández, J.E., 2006. Treatment of
647 biogas produced in anaerobic reactors for domestic wastewater: Odor control and
648 energy/resource recovery. Rev. Environ. Sci. Bio Tech. 5(1), 93–114.
649 https://doi.org/10.1007/s11157-005-2754-6.
650
651 Pelaz, L., Gómez, A., Garralón, G., Letona, A., Fdz-Polanco, M., 2017. Denitrification
652 of the anaerobic membrane bioreactor (AnMBR) effluent with alternative electron
653 donors in domestic wastewater treatment. Bioresour. Tchnol. 43, 1173–1179.
654 https://doi.org/10.1016/j.biortech.2017.06.168.

Randall, C.W., Sen, D., 1996. Full-scale evaluation of an integrated fixed-film activated sludge (IFAS) process for enhanced nitrogen removal. Water Sci. Technol. 33(12), 155–162. https://doi.org/10.1016/0273-1223(96)00469-6.

Rice, E.W., Baird, R.B., Eaton, A.D., Clesceri, L.S., 2012. Standard Methods for the Examination of Water and Wastewater, 22nd edition. American Public Health Association, American Water Works Association and the Water Environment Federation, Washington DC, USA.

Sánchez A., Rodriguez-Hernandez L., Buntner, D., Esteban-García A.L., Tejero I., Garrido, J.M., 2016, Denitrification coupled with methane oxidation in a membrane bioreactor after methanogenic pre-treatment of wastewater. J. Chem. Technol. Biotechnol. 91, 2950–2958. https://doi.org/10.1002/jctb.4913.

Silva-Teira A., Sánchez A., Bunter D., Rodrıíguez-Hernández L., Garrido J.M., 2017. Removal of dissolved methane and nitrogen from anaerobically treated effluents at low temperature by MBR post-treatment. Chem. Eng. J. 326, 970-979. https://doi.org/10.1016/j.cej.2017.06.047.

Van Kessel M.A.H.J., Stultiens, K., Slegers, M.F., Guerrero Cruz, S., Jetten, M.S.M., Kartal, B., Op den Camp, H.J., 2018. Current perspectives on the application of N-damo and anammox in wastewater treatment. Curr. Opin. Biotechnol. 50, 222-227. https://doi.org/10.1016/j.copbio.2018.01.031.

Villaverde, S., Fdz-Polanco, F., García, P.A., 2000. Nitrifying biofilm acclimation to free ammonia in submerged biofilters. Start-up influence. Water Res. 34, 602–610. https://doi.org/10.1016/S0043-1354(99)00175-X.

Welander, U., Henrysson, T., Welander, T., 1998. Biological nitrogen removal from municipal landfill leachate in a pilot scale suspended carrier biofilm process. Water Res. 32(5), 1564-1570. https://doi.org/10.1016/S0043-1354(97)00351-5.

Young, B., Delatolla, R., Kennedy, K., Laflamme, E., Stintzi, A., 2017. Low temperature MBBR nitrification: Microbiome analysis. Water Res. 11, 224-233. https://doi.org/10.1016/j.watres.2016.12.050.

Supplementary Material

1. Mass balances calculations.

The volumetric removal rates of oxygen, methane and nitrogen (mg L^{-1} d^{-1}) were calculated in the anoxic compartment of the IFAS system by applying mass balances (Equation S1). Similarly, methane and nitrogen removal rates were also calculated in the aerobic compartment by means of Equation S2. It was taken into consideration that the approximation to an ideal continuous stirred tank reactor (CSTR) can be applied to both compartments.

$$Removal\ rates = \frac{Q_f.(C_x)_{UASB}+(Q_{R1}+Q_{R2}).(C_x)_{aero}-(Q_f+Q_{R1}+Q_{R2}).(C_x)_{anox}}{V_{anox}} \quad \text{(S1)}$$

$$Removal\ rates = \frac{(Q_f+Q_{R1}+Q_{R2}).(C_{x_{anox}}-C_{x_{aero}})}{V_{aero}} \quad \text{(S2)}$$

Where Q_f is the feeding flow (L d^{-1}) applied to the combined UASB-IFAS system; C_x is the concentration of oxygen, methane and nitrogen in the liquid phase (mg L^{-1}) of each compartment: UASB, aerobic (aero) and anoxic (anox); Q_{R1} is the recirculation flow from the aerobic to the anoxic compartment of the IFAs system (L d^{-1}); Q_{R2} is the recirculation flow from the settler to the anoxic compartment of the IFAS system (L d^{-1}); and V is the compartment volumen (36 and 20 L for anoxic and aerobic, respectively).

However, not all the dissolved methane that was led from the anoxic to the aerobic compartment was biologically oxidized, but a fraction of it could be also stripped-off into the atmosphere. The continuous detection of methane in the aerobic compartment allowed to estimate the amount of methane that was desorbed from the aerobic compartment. To this end, the oxygen volumetric mass transfer coefficient (k_La) was calculated (Equation S3).

$$k\ a_{O_2} = \frac{ORR_{aerobic}}{(DO_{saturation} - DO_{aerobic})} \quad \text{(S3)}$$

Where k_La_{O2} represents the volumetric mass transfer coefficient for oxygen (d^{-1}); ORR, corresponds to the measured oxygen removal rate in the aerobic compartment (mg O_2 L^{-1} d^{-1}); $DO_{saturation}$, represents the estimated dissolved oxygen saturation concentration at the given temperature (mg O_2 L^{-1}); $DO_{aerobic}$, is the dissolved oxygen concentration measured in the aerobic compartment (mg O_2 L^{-1}).

By considering $k_La_{CH4} = 0.8 \cdot k_La_{O2}$ (Sánchez et al., 2016), the methane desorbed in the aerobic compartment can be calculated as follows:

$$CH_{4\ desorbed} = C_{CH_4} \cdot 0.8 \cdot k\ a_{O_2} \quad \text{(S4)}$$

Where $CH_{4desorbed}$ represents the amount of methane desorbed per unit of volume of the aerobic compartment and per unit of time (mg CH_4 L^{-1} d^{-1}) and C_{CH4} is the concentration of methane measured in the aerobic compartment (mg CH_4 L^{-1}).

2. DNA extraction, sequencing and analysis.

To characterize the microbial community, total genomic DNA was extracted using the Biofilm DNA Isolation Kit (Norgen, Thorold, Canada) following the manufacturer instractions. Then, total DNA concentrations were determined using a Qubit fluorometer (Thermo Fisher Scientific, Waltham, MA, USA). DNA size and integrity was tested by standard electrophoresis. The V3V4 region of the bacterial 16S rRNA gene was amplified with the primer pair S-D-Bact-0341-b-S-17 and S-D-Bact-0785-a-A (Klindworth et al. 2013). The V2V3 region of the archaeal 16S rRNA gene was amplified with the primer set Arch1F and Arch1R (Cruaud et al. 2014). For that, an initial amplification was carried out in 25 µL volumes containing 3 ng of total DNA, 100 nM of bacterial primers or 200 nM of archaeal primers, and 1X Q5® High Fidelity Master Mix (New England BioLabs) which contains the DNA polymerase, 2mM $MgCl_2$ and 200 µM dNTPs. PCR conditions were: initial denaturation at 98°C for 30 s followed by 20 (*Bacteria*) or 22 (*Archaea*) cycles (denaturation: 98°C for 10 s, annealing: 50°C for *Bacteria* or 48°C for *Archaea* during 20 s, extension: 72°C for 20 s); followed by an extension step of 2 min at 72°C. A second PCR was used to add the Illumina adapters and barcodes to the amplicons. The conditions were similar to the first PCR but in this case, only 15 cycles were applied and the annealing temperature was 60°C. Library DNA concentration was then determined in a Bioanalyzer (Bioanalyzer, Agilent Technologies, Santa Clara, CA, USA). Libraires were pooled in equimolar amounts and sequenced in a MiSeq Illumina sequencer (Illumina, Inc.) at Unidad de

749 Genómica, Parque Científico de Madrid. Paired-end reads (2x300) were generated
750 following manufacturer protocols (Illumina, Inc.).

751 Obtained sequences were de-multiplexed and trimmed to remove Illumina adapters,
752 barcodes. In addition, the last 50 pb of the 5' ends were removed due to the low-quality
753 scores (Q<30). Next, paired-end reads were merged as previously described (Eren et al.
754 2013) filtering sequences with quality scores below Q30 and a minimum overlap of 50
755 bp. In addition, all sequences containing indeterminations were removed from further
756 analysis. The obtained high-quality sequences, were analyzed with VSEARCH in de
757 novo mode for chimera removal (Rognes et al. 2016) and clustered into Operational
758 Taxonomic Units (OTUs) using the 97% cutoff for sequences similarity using QIIME
759 (Caporaso et al. 2010). OTUs taxonomic affiliation was determined with USEARCH
760 (Edgar 2010) with the Greengenes database version 13 8 (DeSantis et al. 2006).

761

762 **3. References**

763 Caporaso, J.G., Kuczynski, J., Stombaugh, J., Bittinger, K., Bushman, F.D., Costello,
764 E.K., Fierer, N., Peña, A.G., Goodrich, J.K., Gordon, J.I., Huttley, G.A., Kelley, S.T.,
765 Knights, D., Koenig, J.E., Ley, R.E., Lozupone, C.A., Mcdonald, D., Muegge, B.D.,
766 Pirrung, M., Reeder, J., Sevinsky, J.R., Turnbaugh, P.J., Walters, W.A., Widmann, J.,
767 Yatsunenko, T., Zaneveld, J., Knight, R., 2010. QIIME allows analysis of high-
768 throughput community sequencing data. Nat. Methods 7, 335–336.
769 https://doi.org/10.1038/nmeth0510-335.

770

771 Cruaud, P., Vigneron, A., Lucchetti-Miganeh, C., Ciron, P.E., Godfroy, A., Cambon-
772 Bonavita, M.A., 2014. Influence of DNA extraction method, 16S rRNA targeted

773 hypervariable regions, and sample origin on microbial diversity detected by 454
774 pyrosequencing in marine chemosynthetic ecosystems. Appl. Environ. Microbiol. 80,
775 4626–4639. https://doi.org/10.1128/AEM.00592-14.
776
777 DeSantis, T.Z., Hugenholtz, P., Larsen, N., Rojas, M., Brodie, E.L., Keller, K., Huber,
778 T., Dalevi, D., Hu, P., Andersen, G.L. 2006. Greengenes, a chimera-checked 16S rRNA
779 gene database and workbench compatible with ARB. Appl. Environ. Microbiol. 72,
780 5069–5072. https://doi.org/10.1128/AEM.03006-05.
781
782 Edgar, R.C., 2010. Search and clustering orders of magnitude faster than BLAST.
783 Bioinformatics 26, 2460–2461. https://doi.org/10.1093/bioinformatics/btq461.
784
785 Eren, A.M., Vineis, J.H., Morrison, H.G., Sogin, M.L., 2013. A filtering method to
786 generate high quality short reads using Illumina paired-end technology. PLOS One 8(6),
787 e66643. https://doi.org/10.1371/journal.pone.0066643.
788
789 Klindworth, A., Pruesse, E., Schweer, T., Peplies, J., Quast, C., Horn, M., Glöckner,
790 F.O., 2013. Evaluation of general 16S ribosomal RNA gene PCR primers for classical
791 and next-generation sequencing-based diversity studies. Nucleic Acids Res. 41, 1–11.
792 https://doi.org/ 10.1093/nar/gks808.
793
794 Rognes., T., Flouri, T., Nichols, B., Quince, C., Mahé, F., 2016. VSEARCH: a versatile
795 open source tool for metagenomics. Peer J. 4, e2584. https://doi.org/10.7717/peerj.2584.
796

797 Sánchez A., Rodriguez-Hernandez L., Buntner, D., Esteban-García A.L., Tejero I.,
798 Garrido, J.M., 2016, Denitrification coupled with methane oxidation in a membrane
799 bioreactor after methanogenic pre-treatment of wastewater. J. Chem. Technol.
800 Biotechnol. 91, 2950–2958. https://doi.org/10.1002/jctb.4913.

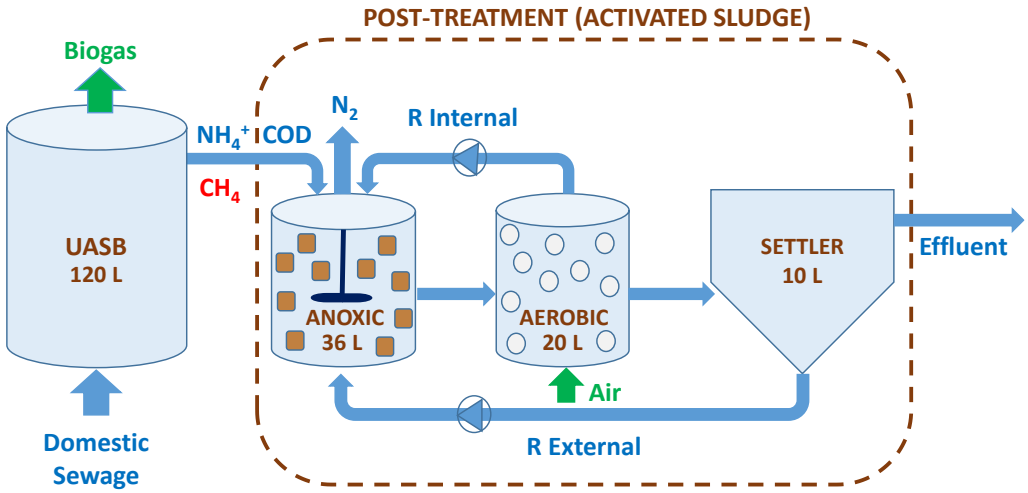
POST-TREATMENT (ACTIVATED SLUDGE)
Biogas
UASB
120 L
NH_4^+
COD
CH_4
N_2
R Internal
ANOXIC
36 L
AEROBIC
20 L
Air
SETTLER
10 L
Effluent
R External
Domestic
Sewage

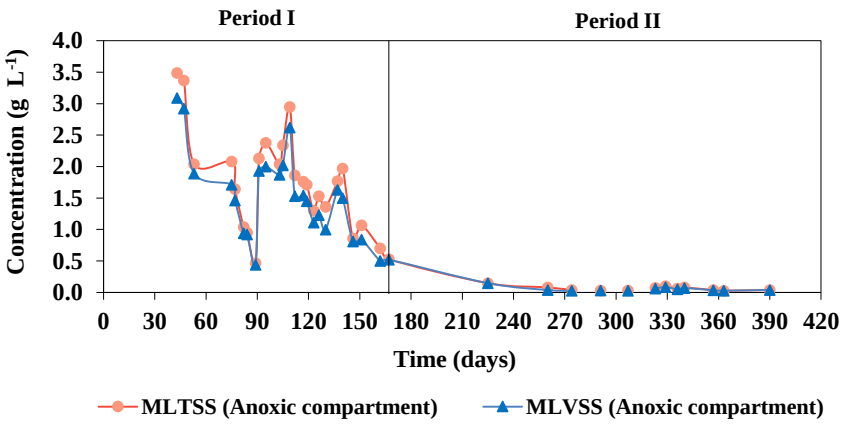
Period I
Period II
Concentration (g L-1)
4.0
3.5
3.0
2.5
2.0
1.5
1.0
0.5
0.0
0
30
60
90
120
150
180
210
240
270
300
330
360
390
420
Time (days)
MLTSS (Anoxic compartment)
MLVSS (Anoxic compartment)

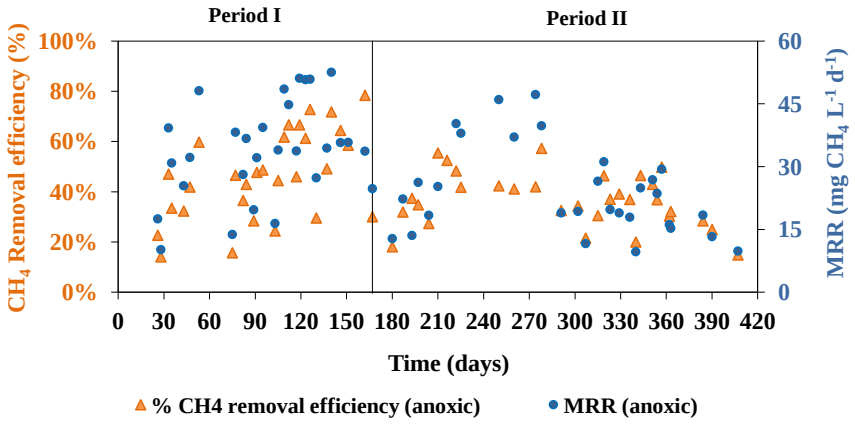
Period I
Period II
CH4 Removal efficiency (%)
100%
80%
60%
40%
20%
0%
MRR (mg CH4 L-1 d-1)
60
45
30
15
0
0 30 60 90 120 150 180 210 240 270 300 330 360 390 420
Time (days)
% CH4 removal efficiency (anoxic)
MRR (anoxic)

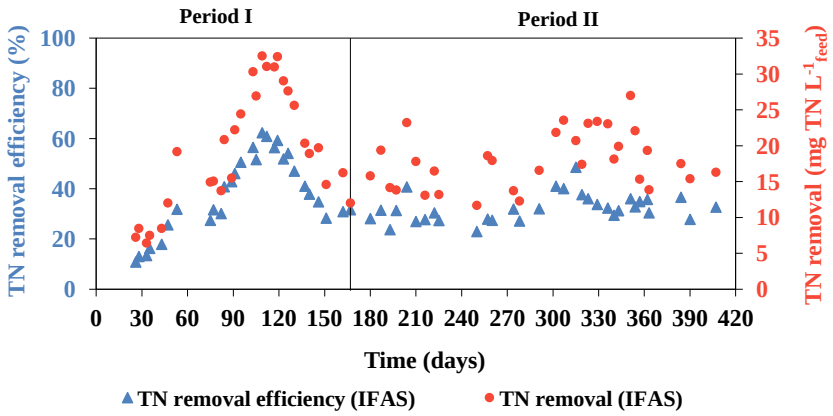
Period I
Period II
TN removal efficiency (%)
TN removal (mg TN L-1feed)
0
20
40
60
80
100
0
5
10
15
20
25
30
35
0 30 60 90 120 150 180 210 240 270 300 330 360 390 420
Time (days)
TN removal efficiency (IFAS)
TN removal (IFAS)

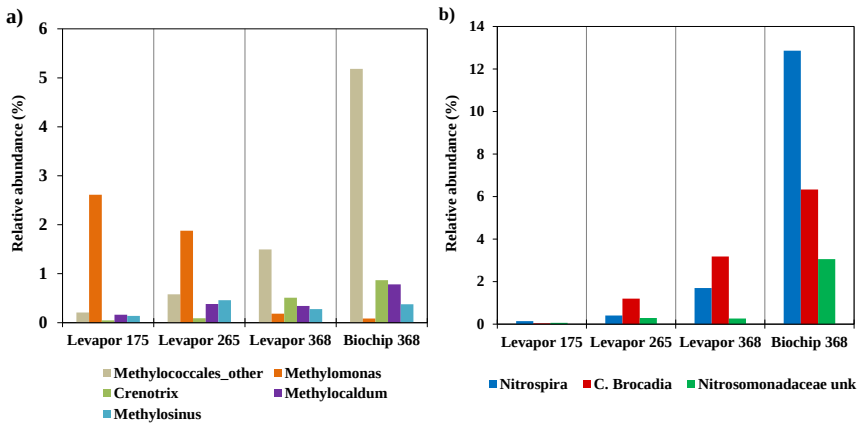
a)
Relative abundance (%)
0
1
2
3
4
5
6
Levapor 175
Levapor 265
Levapor 368
Biochip 368
Methylococcales_other
Methylomonas
Crenotrix
Methylocaldum
Methylosinus
b)
Relative abundance (%)
0
2
4
6
8
10
12
14
Levapor 175
Levapor 265
Levapor 368
Biochip 368
Nitrospira
C. Brocadia
Nitrosomonadaceae unk

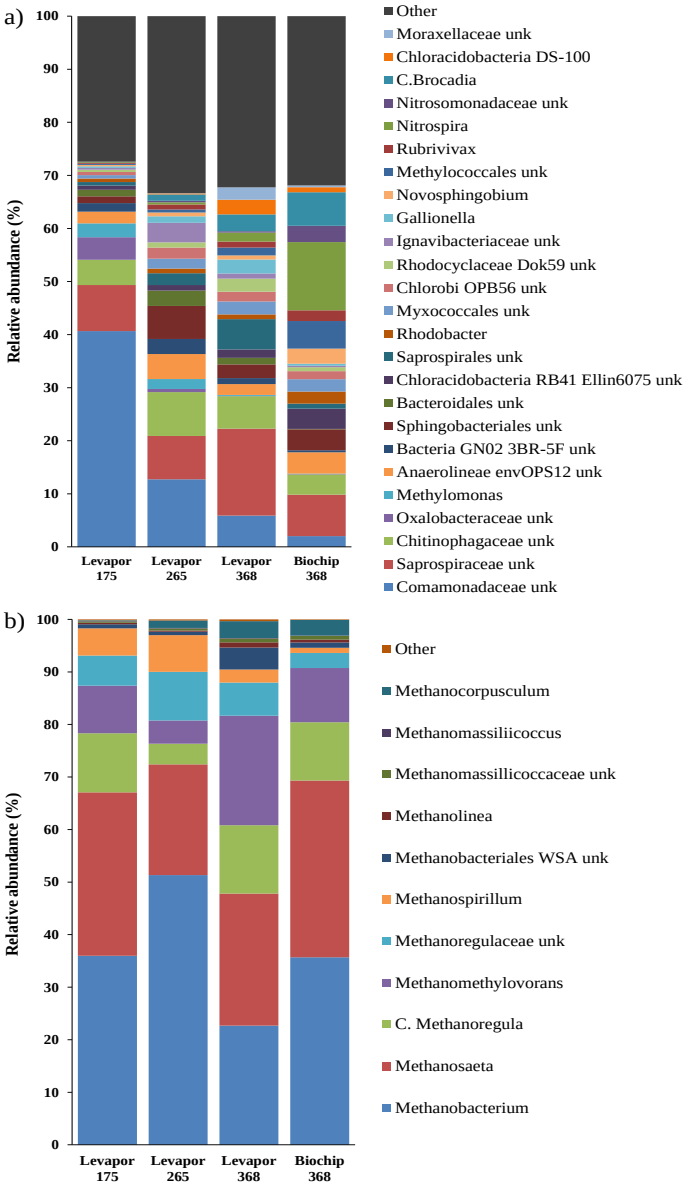
a)
Relative abundance (%)
100
90
80
70
60
50
40
30
20
10
0
Levapor 175
Levapor 265
Levapor 368
Biochip 368
Other
Moraxellaceae unk
Chloracidobacteria DS-100
C.Brocadia
Nitrosomonadaceae unk
Nitrospira
Rubrivivax
Methylococcales unk
Novosphingobium
Gallionella
Ignavibacteriaceae unk
Rhodocyclaceae Dok59 unk
Chlorobi OPB56 unk
Myxococcales unk
Rhodobacter
Saprospirales unk
Chloracidobacteria RB41 Ellin6075 unk
Bacteroidales unk
Sphingobacteriales unk
Bacteria GN02 3BR-5F unk
Anaerolineae envOPS12 unk
Methylomonas
Oxalobacteraceae unk
Chitinophagaceae unk
Saprospiraceae unk
Comamonadaceae unk
b)
Relative abundance (%)
100
90
80
70
60
50
40
30
20
10
0
Levapor 175
Levapor 265
Levapor 368
Biochip 368
Other
Methanocorpusculum
Methanomassiliicoccus
Methanomassillicoccaceae unk
Methanolinea
Methanobacteriales WSA unk
Methanospirillum
Methanoregulaceae unk
Methanomethylovorans
C. Methanoregula
Methanosaeta
Methanobacterium

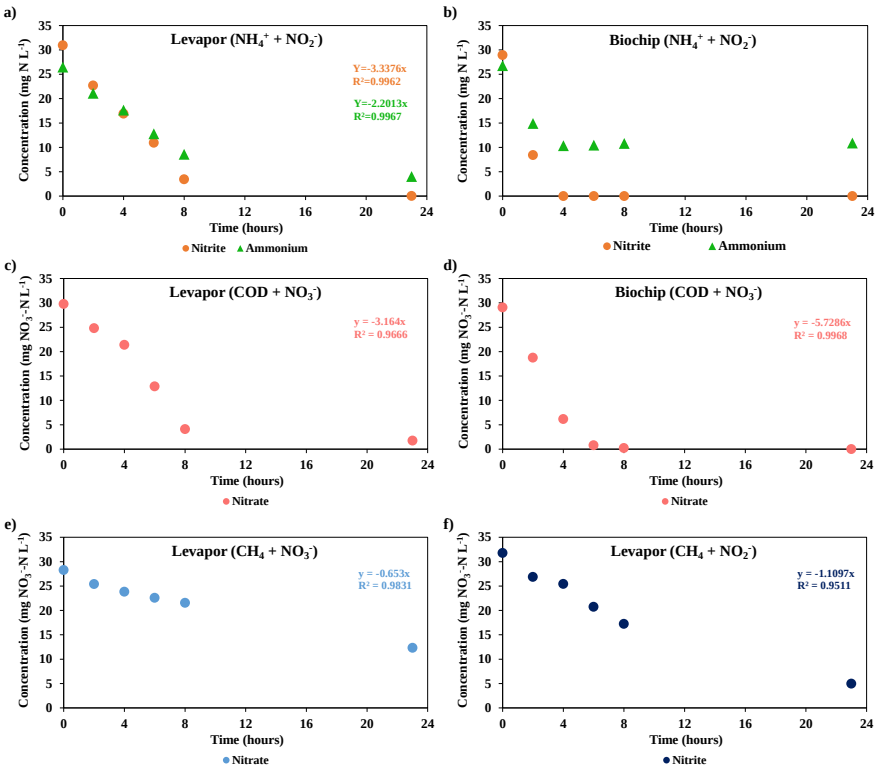
a)
Levapor ($NH_4^+ + NO_2^-$)
Y=-3.3376x
R²=0.9962
Y=-2.2013x
R²=0.9967
Concentration (mg N L⁻¹)
Time (hours)
Nitrite
Ammonium
b)
Biochip ($NH_4^+ + NO_2^-$)
Concentration (mg N L⁻¹)
Time (hours)
Nitrite
Ammonium
c)
Levapor (COD + NO_3^-)
y = -3.164x
R² = 0.9666
Concentration (mg NO_3^--N L⁻¹)
Time (hours)
Nitrate
d)
Biochip (COD + NO_3^-)
y = -5.7286x
R² = 0.9968
Concentration (mg NO_3^--N L⁻¹)
Time (hours)
Nitrate
e)
Levapor ($CH_4 + NO_3^-$)
y = -0.653x
R² = 0.9831
Concentration (mg NO_3^--N L⁻¹)
Time (hours)
Nitrate
f)
Levapor ($CH_4 + NO_2^-$)
y = -1.1097x
R² = 0.9511
Concentration (mg NO_3^--N L⁻¹)
Time (hours)
Nitrite

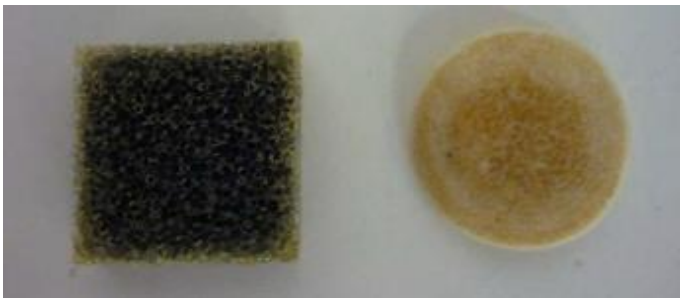

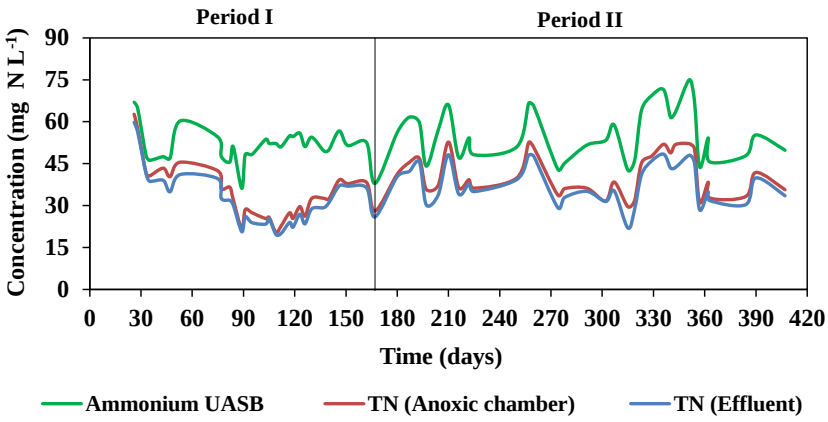
Period I
Period II
Concentration (mg N L-1)
90
75
60
45
30
15
0
0
30
60
90
120
150
180
210
240
270
300
330
360
390
420
Time (days)
Ammonium UASB
TN (Anoxic chamber)
TN (Effluent)

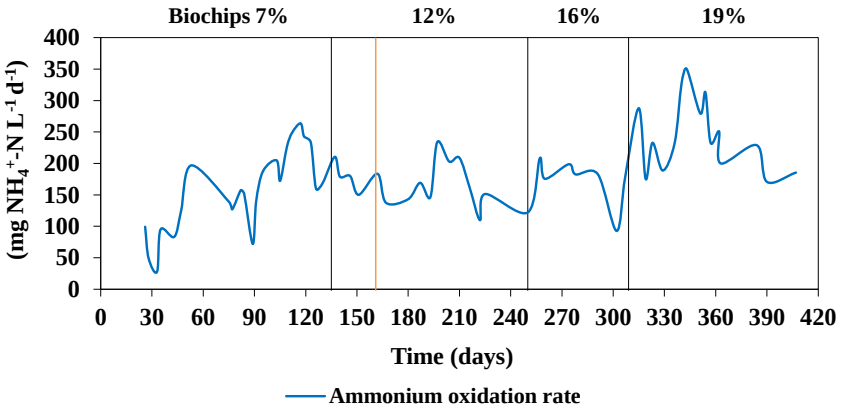
Biochips 7%
12%
16%
19%
400
350
300
250
200
150
100
50
0
(mg NH_4^+-N L^{-1} d^{-1})
0
30
60
90
120
150
180
210
240
270
300
330
360
390
420
Time (days)
Ammonium oxidation rate

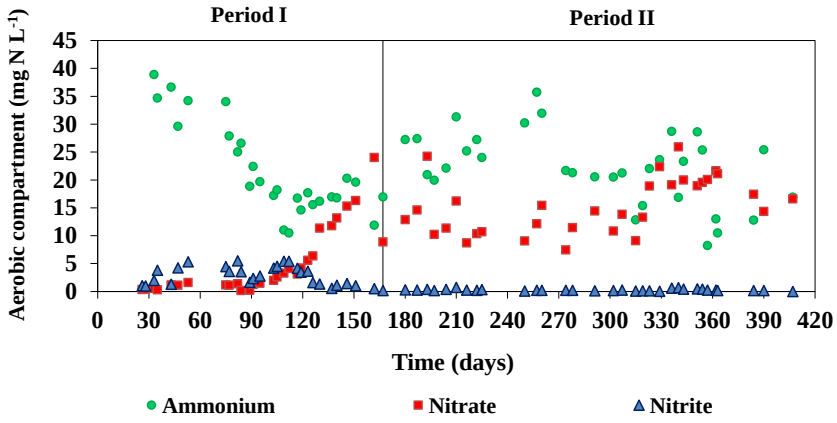
Period I
Period II
Aerobic compartment (mg N L-1)
45
40
35
30
25
20
15
10
5
0
0
30
60
90
120
150
180
210
240
270
300
330
360
390
420
Time (days)
Ammonium
Nitrate
Nitrite

Figure 1. Schematic diagram of the UASB methanogenic reactor coupled to an IFAS post-treatment system.

Figure 2. Evolution of the mixed-liquor total (MLTSS) and volatile (MLTVSS) suspended solids concentration in the anoxic compartment.

Figure 3. Evolution of methane removal efficiencies and volumetric methane removal rates (MRR) in the pre-anoxic compartment of the IFAS system.

Figure 4. Evolution of TN removal efficiencies and TN removal observed in the IFAS post-treatment system throughout the operating period.

Figure 5. Relative abundances of aerobic methanotrophs (a) and of the most abundant nitrifying and anammox bacteria (b) in the Levapor (days 175, 265 and 368) and Biochips (day 368) carriers. Only the aerobic methanotrophos with relative abundances over 0.5% in at least one observation are shown.

Figure 6. a) Relative abundances of the 25 most dominant bacteria in the Levapor carriers on days 175, 265 and 368; and in the Biochip carriers on day 368 and b) Composition of the archaeal community in the Levapor and Biochip carriers. Numbers indicate the operational day.

Figure 7. Batch denitrification tests results for anammox process in Levapor (a) and Biochip (b) carriers media; for conventional heterotrophic denitrification in Levapor (c) and Biochip (d); and anaerobic methane oxidation processes in Levapor using nitrate (e) and nitrite (f) as electron acceptor.

Figure S1. Real image of the used UASB-IFAS integrated system (pilot plant).

Figure S2. Sponge Levapor (left) and rigid-plastic Biochip (right) biofilm carriers.

Figure S3. Evolution of the ammonium concentration fed to the IFAS system and the measured TN ions concentration in the anoxic compartment and the IFAs effluent.

Figure S4. Evolution of the ammonium oxidation rates observed in the aerobic compartment of the IFAS system. Black lines separate periods of time according to the apparent volume of the Biochip carriers (%). The orange line separates Period I from Period II.

Figure S5. Evolution of different nitrogen species in the aerobic compartment of the post-treatment system.

***Author Contributions Section**

CRediT author statement

Tomás Allegue: investigation, writing original draft, formal analysis, conceptualization; **María Nieves Carballo-Costa**: investigation, methodology; **Nuria Fernández González**: methodology, formal analysis, investigation; **Juan Manuel Garrido Fernández**: conceptualization, funding acquisition, supervision, project administration.